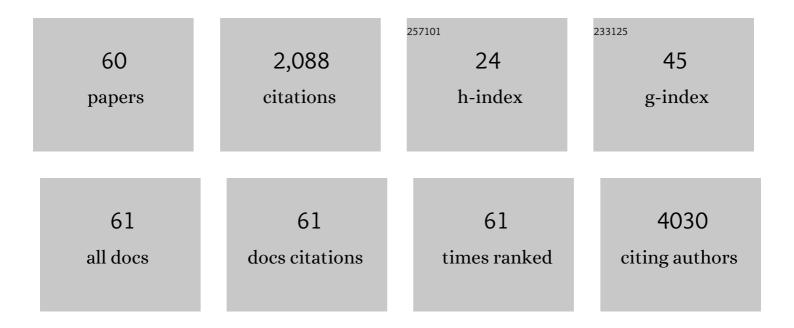
Seong Chu Lim

List of Publications by Year in descending order

Source: https://exaly.com/author-pdf/2754453/publications.pdf Version: 2024-02-01



#	Article	IF	CITATIONS
1	Gate tunable photoresponse of a two-dimensional p-n junction for high performance broadband photodetector. Applied Materials Today, 2022, 26, 101285.	2.3	7
2	ldentifying the Origin of Defect-Induced Raman Mode in WS ₂ Monolayers via Density Functional Perturbation Theory. Journal of Physical Chemistry C, 2022, 126, 4182-4187.	1.5	4
3	Correlation of Defect-Induced Photoluminescence and Raman Scattering in Monolayer WS ₂ . Journal of Physical Chemistry C, 2022, 126, 7177-7183.	1.5	8
4	Optical Duality of Molybdenum Disulfide: Metal and Semiconductor. Nano Letters, 2022, 22, 5207-5213.	4.5	7
5	Enhanced Electron Heat Conduction in TaS3 1D Metal Wire. Materials, 2021, 14, 4477.	1.3	2
6	Ultrasensitive Photodetection in MoS ₂ Avalanche Phototransistors. Advanced Science, 2021, 8, e2102437.	5.6	34
7	Crossover between thermo- and field-assisted carrier injection in staggered pn heterojunction of MoTe2 and ReS2. Applied Surface Science, 2021, 558, 149870.	3.1	1
8	Quasi-2D Halide Perovskite Memory Device Formed by Acid–Base Binary Ligand Solution Composed of Oleylamine and Oleic Acid. ACS Applied Materials & Interfaces, 2021, 13, 40891-40900.	4.0	10
9	Investigation of Cation Exchange Behaviors of FAxMA1â^'xPbI3 Films Using Dynamic Spin-Coating. Materials, 2021, 14, 6422.	1.3	0
10	Probing Pathways of Conductive Filaments of FAMAPbI ₃ with Controlled FA Composition Using Conductive Atomic Force Microscopy. Journal of Physical Chemistry C, 2021, 125, 25067-25074.	1.5	1
11	Effects of Surface Modifications to Single and Multilayer Graphene Temperature Coefficient of Resistance. ACS Applied Materials & Interfaces, 2020, 12, 48890-48898.	4.0	5
12	Thickness effect on low-power driving of MoS2 transistors in balanced double-gate fields. Nanotechnology, 2020, 31, 255201.	1.3	2
13	Wiedemann-Franz law of Cu-coated carbon fiber. Carbon, 2020, 162, 339-345.	5.4	11
14	Temperature-Dependent Opacity of the Gate Field Inside MoS2 Field-Effect Transistors. ACS Applied Materials & Interfaces, 2019, 11, 29022-29028.	4.0	7
15	Impact of Heat Treatment on a Hetero-Stacked MoS ₂ /\${h}\$ -BN Field-Effect Transistor. IEEE Electron Device Letters, 2019, 40, 1626-1629.	2.2	1
16	Reduced interfacial fluctuation leading enhanced mobility in a monolayer MoS ₂ DG FET under low vertical electric field. Nanotechnology, 2019, 30, 345206.	1.3	7
17	Semimetallic Graphene for Infrared Sensing. ACS Applied Materials & amp; Interfaces, 2019, 11, 19565-19571.	4.0	12
18	Modulating the Functions of MoS ₂ /MoTe ₂ van der Waals Heterostructure	7.3	85

SEONG CHU LIM

#	Article	IF	CITATIONS
19	Defect-Affected Photocurrent in MoTe ₂ FETs. ACS Applied Materials & Interfaces, 2019, 11, 10068-10073.	4.0	19
20	Unsaturated Drift Velocity of Monolayer Graphene. Nano Letters, 2018, 18, 1575-1581.	4.5	13
21	Adhesion Energies of 2D Graphene and MoS ₂ to Silicon and Metal Substrates. Physica Status Solidi (A) Applications and Materials Science, 2018, 215, 1700512.	0.8	37
22	Synthesis and Characterization of Bandgap-modulated Organic Lead Halide Single Crystals. Journal of the Korean Physical Society, 2018, 73, 1716-1724.	0.3	4
23	Gas adsorbates are Coulomb scatterers, rather than neutral ones, in a monolayer MoS ₂ field effect transistor. Nanoscale, 2018, 10, 10856-10862.	2.8	7
24	Ultrafast nonlinear travel of hot carriers driven by high-field terahertz pulse. Journal of Physics B: Atomic, Molecular and Optical Physics, 2018, 51, 144003.	0.6	15
25	Parameter control for enhanced peak-to-valley current ratio in a MoS ₂ /MoTe ₂ van der Waals heterostructure. Nanoscale, 2018, 10, 12322-12329.	2.8	25
26	Thickness-dependent in-plane thermal conductivity of suspended MoS ₂ grown by chemical vapor deposition. Nanoscale, 2017, 9, 2541-2547.	2.8	86
27	Understanding Coulomb Scattering Mechanism in Monolayer MoS ₂ Channel in the Presence of <i>h</i> -BN Buffer Layer. ACS Applied Materials & Interfaces, 2017, 9, 5006-5013.	4.0	37
28	Junction-Structure-Dependent Schottky Barrier Inhomogeneity and Device Ideality of Monolayer MoS ₂ Field-Effect Transistors. ACS Applied Materials & Interfaces, 2017, 9, 11240-11246.	4.0	57
29	Thickness-dependent carrier mobility of ambipolar MoTe2: Interplay between interface trap and Coulomb scattering. Applied Physics Letters, 2017, 110, .	1.5	42
30	Charge Transport in MoS ₂ /WSe ₂ van der Waals Heterostructure with Tunable Inversion Layer. ACS Nano, 2017, 11, 3832-3840.	7.3	175
31	Photocurrent Switching of Monolayer MoS ₂ Using a Metal–Insulator Transition. Nano Letters, 2017, 17, 673-678.	4.5	31
32	Tuning Carrier Tunneling in van der Waals Heterostructures for Ultrahigh Detectivity. Nano Letters, 2017, 17, 453-459.	4.5	178
33	Transient Carrier Cooling Enhanced by Grain Boundaries in Graphene Monolayer. ACS Applied Materials & Interfaces, 2017, 9, 41026-41033.	4.0	6
34	Graphene-CdSe quantum dot hybrid as a platform for the control of carrier temperature. FlatChem, 2017, 6, 77-82.	2.8	9
35	Tunable Mobility in Double-Gated MoTe ₂ Field-Effect Transistor: Effect of Coulomb Screening and Trap Sites. ACS Applied Materials & Interfaces, 2017, 9, 29185-29192.	4.0	31
36	Unraveled Face-Dependent Effects of Multilayered Graphene Embedded in Transparent Organic Light-Emitting Diodes. ACS Applied Materials & Interfaces, 2017, 9, 43105-43112.	4.0	9

SEONG CHU LIM

#	Article	IF	CITATIONS
37	In situ multi-dimensional actuation measurement method for tensile actuation of paraffin-infiltrated multi-wall carbon nanotube yarns. Review of Scientific Instruments, 2017, 88, 075001.	0.6	3
38	Phase conversion of chemically exfoliated molybdenum disulfide. Current Applied Physics, 2017, 17, 60-65.	1.1	12
39	Suppression of Interfacial Current Fluctuation in MoTe ₂ Transistors with Different Dielectrics. ACS Applied Materials & Interfaces, 2016, 8, 19092-19099.	4.0	35
40	Metal-coated carbon fiber for lighter electrical metal wires. Synthetic Metals, 2016, 222, 180-185.	2.1	13
41	Electron Excess Doping and Effective Schottky Barrier Reduction on the MoS ₂ / <i>h</i> -BN Heterostructure. Nano Letters, 2016, 16, 6383-6389.	4.5	78
42	Torsional Actuator Powered by Environmental Energy Harvesting from Diurnal Temperature Variation. ACS Sustainable Chemistry and Engineering, 2016, 4, 6647-6652.	3.2	8
43	Flexion bonding transfer of multilayered graphene as a top electrode in transparent organic light-emitting diodes. Scientific Reports, 2015, 5, 17748.	1.6	35
44	Paper No S4.4: Colored OLED With a Multilayered Graphene Electrode for Light-Adaptable Displays. Digest of Technical Papers SID International Symposium, 2015, 46, 20-20.	0.1	0
45	Modulating the shape of ZnO nanostructures grown by using thermal chemical-vapor deposition. Journal of the Korean Physical Society, 2015, 67, 1588-1591.	0.3	1
46	Sensitive photo-thermal response of graphene oxide for mid-infrared detection. Nanoscale, 2015, 7, 15695-15700.	2.8	57
47	Positive gate bias stress instability of carbon nanotube thin film transistors. Applied Physics Letters, 2012, 101, 053504.	1.5	17
48	Heat Dissipation of Transparent Graphene Defoggers. Advanced Functional Materials, 2012, 22, 4819-4826.	7.8	238
49	Humidity-assisted selective reactivity between NO2 and SO2 gas on carbon nanotubes. Journal of Materials Chemistry, 2011, 21, 4502.	6.7	54
50	Facile Physical Route to Highly Crystalline Graphene. Advanced Functional Materials, 2011, 21, 3496-3501.	7.8	97
51	Contact resistance between metal and carbon nanotube interconnects: Effect of work function and wettability. Applied Physics Letters, 2009, 95, .	1.5	184
52	Origin of enhanced field emission characteristics postplasma treatment of multiwalled carbon nanotube array. Applied Physics Letters, 2008, 93, 063101.	1.5	13
53	Photocurrent of CdSe nanocrystals on single-walled carbon nanotube-field effect transistor. Applied Physics Letters, 2008, 92, .	1.5	22
54	Terahertz optical and electrical properties of hydrogen-functionalized carbon nanotubes. Physical Review B, 2007, 75, .	1.1	52

SEONG CHU LIM

#	Article	IF	CITATIONS
55	A diameter-selective chiral separation of single-wall carbon nanotubes using nitronium lons. Journal of Electronic Materials, 2006, 35, 235-242.	1.0	18
56	Preferential etching of metallic single-walled carbon nanotubes with small diameter by fluorine gas. Physical Review B, 2006, 73, .	1.1	74
57	Nanomanipulator-assisted fabrication and characterization of carbon nanotubes inside scanning electron microscope. Micron, 2005, 36, 471-476.	1.1	28
58	Frequency-dependent optical constants and conductivities of hydrogen-functionalized single-walled carbon nanotubes. Applied Physics Letters, 2005, 87, 041908.	1.5	28
59	Electrical and Optical Properties of Carbon Nanotubes Characterized by Terahertz Electromagnetic Pulses. , 2005, , .		0
60	In situmanipulation and characterizations using nanomanipulators inside a field emission-scanning electron microscope. Review of Scientific Instruments, 2003, 74, 4021-4025.	0.6	34